Cement and Concrete Research 106 (2018) 40–48

Contents lists available at ScienceDirect

Cement and Concrete Research

journal homepage: www.elsevier.com/locate/cemconres

Determination of the amount of reacted metakaolin in calcined clay blends

François Avet*, Xuerun Li, Karen Scrivener

Laboratory of Construction Materials, IMX, EPFL, 1015 Lausanne, Switzerland

ARTICLE INFO

Keywords:
Calcined clay
Metakaolin
Mass balance
Thermodynamic modelling
PONKCS

ABSTRACT

This paper presents a comparative study of three methods to determine the amount of reacted metakaolin in calcined clay blends: mass balance, thermodynamic modelling, and the Partial or not Known Crystalline Structure method (PONKCS) based on Rietveld analysis of X-ray diffraction. The methods are applied to Limestone calcined clay cements (LC^3-50) in this study. Mass balance and thermodynamic modelling results show good agreement, especially at early age. PONKCS method shows globally comparable results, even if it has higher variability. The precision of PONKCS becomes poor for blends with < 60% of metakaolin in calcined clay.

1. Introduction

Calcined clays are receiving increasing attention as supplementary cementitious materials (SCMs). The supplies of traditional SCMs (fly ash and slag) are limited compared to the amount of clinker produced. The most widely available materials able to meet at reasonable cost the increasing demand of cement production are limestone and calcined kaolinitic clays [1]. Kaolinitic clays show the highest pozzolanic activity after calcination among the different kinds of clays, thanks to the formation of the highly reactive amorphous metakaolin phase [2–5]. There have been numerous previous studies on the use of pure metakaolin, but clays with a lower kaolinite content are much more promising for massive use in cement due to their wide availability, and low cost. Of special interest is the co-substitution of clinker by calcined clay and limestone as in Limestone Calcined Clay Cements (LC^3)[1] [6]. A method to measure the degree of reaction of metakaolin for these various grades of calcined clays is a key step to better understand the influence of the grade of clay on the properties of cementitious blends containing calcined clays.

Methods for the determination of the reaction degree of SCMs were reviewed by Scrivener and al. [7].

- Nuclear Magnetic Resonance (^{27}Al and ^{29}Si) can be used with a good accuracy [8–10]. However, this technique is not readily available, it is expensive and a major issue is the presence of paramagnetic iron ions (Fe^{3+}) [11] coming from cement and in impure calcined clays, where iron oxides are frequently found as secondary phase but also in substitution within the clay structure. These ions are responsible for decreasing the magnetization during the experiment, impacting the reliability of the results.
- Image analysis cannot be used to accurately quantify the amount of reacted metakaolin due to the fine nature of calcined clay particles.
- Calorimetry was thought to be a promising method, but Berodier [12] showed that the long term reaction of the clinker is affected by reactive SCMs so errors are produced when the output is compared to that of an inert material. Moreover, the specific heat of hydration of metakaolin reaction is unknown.
- Antoni and al. [13] estimated the degree of reaction of metakaolin from the portlandite consumption. However, his method underestimates the real reaction degree of metakaolin, because it is assumed that the C-A-S-H composition measured is only related to the reaction of metakaolin. This method does not take into account the change in composition of the C-A-S-H coming from the reaction of clinker [14].

In this study, three methods are compared to determine the amount of reacted metakaolin. First, a global mass balance is investigated considering all the phases involved during hydration, as proposed by Durdzinski et al. [15], but with a fitting for the reaction degree of metakaolin. Using the same inputs as mass balance, a thermodynamic modelling approach is used with the Gibbs Free Energy Minimization Software (GEMS). Finally, the Partial or not Known Crystalline Structure method (PONKCS) based on XRD Rietveld analysis is used, which showed promising results on high-grade metakaolin [16].

This paper is the precursor to another detailing the microstructural evolution in LC^3-50 systems (LC^3 with a clinker content decreased to 50%), which discusses in more detail the evolution of all the hydrates phases and the porosity [17].

* Corresponding author.
E-mail address: francois.avet@epfl.ch (F. Avet).
[1] LC^3: Limestone Calcined Clay Cement: http://www.lc3.ch.

https://doi.org/10.1016/j.cemconres.2018.01.009
Received 22 August 2017; Received in revised form 5 January 2018; Accepted 10 January 2018

2. Methods

2.1. Mass balance

"Mass balance" is a method for calculating the hydrated phase assemblage. The amounts of each oxide coming from the reacted anhydrous phases are redistributed between the hydrate phases known to form [18]. The amount of reacted components coming from clinker phases, limestone and gypsum was considered. Since the reaction degree of metakaolin AS_2 is unknown, its amount is the free variable of the system. It is determined from the best agreement of the mass balance outputs with experimental data.

The sum of the different oxides coming from all the reacting phases are considered: CaO, SiO_2, Al_2O_3, Fe_2O_3, SO_3, CO_2 and MgO. Then a series of steps are used to calculate the amounts of the different phases formed, analogous to the Bogue calculation for the anhydrous phases in Portland cement. The sequence of steps is as follows and schematized in Fig. 1:

- All MgO is considered to form hydrotalcite like phase M_4AH_{10} (Hg), subtracting the Al_2O_3 contribution from the initial Al_2O_3 amount available for the formation of hydration products.
- All Fe_2O_3 is then considered to form Fe-siliceous hydrogarnet $C_3FS_{0.84}H_{4.32}$ (Ht), which is more stable than Fe-ettringite and Fe-AFm phases [19]. The required amounts of silicon and calcium oxides used for hydrogarnet formation are subtracted from their initial available content.
- All the remaining SiO_2 is then considered to be in C-A-S-H. Knowing the Al/Ca, Si/Ca ratios for the different systems at all ages by Scanning Electron Microscopy in Energy Dispersive X-ray Spectroscopy mode (SEM-EDX), the aluminium and calcium contributions are subtracted.
- The quantity of ettringite $C_3A.3(C\$)H_{32}$ (AFt) is taken as that measured by X-ray Diffraction - Rietveld method and from this the amounts of SO_3, CaO and Al_2O_3 are subtracted. Another strategy would consist of consuming all SO_3 for the formation of ettringite. But this leads to errors due to the sulfate adsorption on C-A-S-H.
- The remaining Al_2O_3 is used for the formation of monocarboaluminate $C_4A\underline{C}H_{11}$ (Mc), consuming the available CO_2. Al_2O_3 was used as the limiting factor of the reaction rather than CO_2 because of the relative difficulty for the quantification of calcite by XRD-Rietveld.
- The amount of remaining CaO is used to form portlandite (CH).

With the increase of the metakaolin reaction, extra SiO_2 and Al_2O_3 are provided to the system. To determine the amount of reacted metakaolin, calculations are made at steps of 1% metakaolin reaction and then plotted against the amount of portlandite. The real amount of metakaolin reactions can then be estimated from the portlandite content measured by XRD-Rietveld results.

2.2. Thermodynamic modelling

For thermodynamic modelling, the same oxide contributions as mass balance are used as an input. The Gibbs Free Energy Minimization Software (GEMS) is used [20], with the Cemdata14 database [21] and the CSHQ model from Kulik for C-S-H [22]. Al-incorporation in C-A-S-H was fixed for each system based the Al/Si ratio obtained by SEM-EDX point analysis. According to recent results by ^{1}H NMR from Müller [23], the density of C—S—H used is 2.00 g.cm^{-3}. Moreover, 4 water molecules per silicate ion were considered. Thus, the amount of C-A-S-H and water given by thermodynamic modelling are corrected to include the same water content as the C-A-S-H used by mass balance. As for mass balance, the amount of reacted metakaolin was determined when the same portlandite content as experimental XRD-Rietveld was obtained.

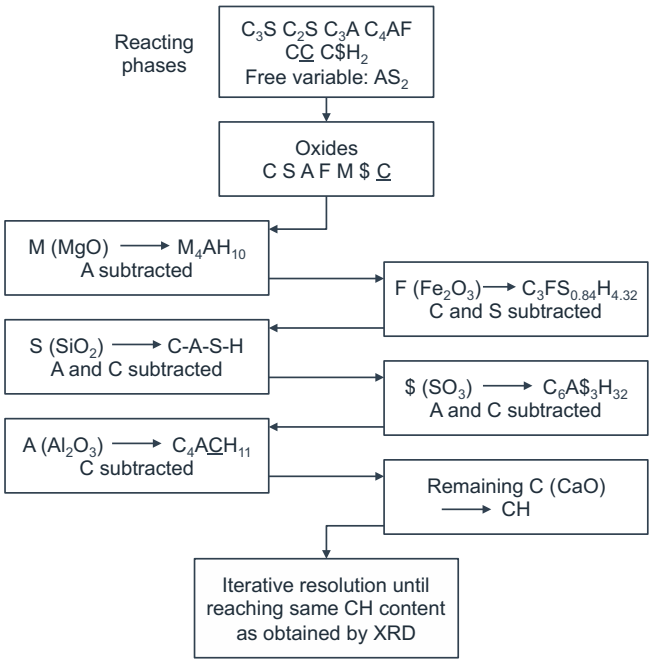

Fig. 1. Mass balance procedure.

2.3. PONKCS method

The traditional use of XRD-Rietveld analysis is limited to the quantification of crystalline phases and the total amorphous content. For hydrated calcined clay blended cement, the amorphous part is mainly composed of C-A-S-H and unreacted metakaolin. The quantification of the distinct amorphous humps from these two phases is made possible by the PONKCS method [14, 16, 18].

Using Rietveld analysis, the weight content of a phase α can be obtained according to Eq. (1), by comparing the scale factor S_α to the scale factor of the external standard S_{std} measured under the same conditions. The differences of phase density ρ and volume V between the phase α and the rutile are considered, as well as the different mass absorption coefficients μ.

$$w_\alpha = \frac{S_\alpha (\rho V^2)_\alpha \mu_{mix} w_{std}}{S_{std} (\rho V^2)_{std} \mu_{std}} \quad (1)$$

For amorphous materials, the phase constants are unknown. The phase constants can be calibrated according to Eq. (2), where a sample composed of a known quantity of amorphous material is analysed. The phase volume is set to 1 to simplify the calculation, leaving ρ_{Ponkcs} as the only unknown of the system.

$$\rho_{Ponkcs} V = \frac{K_{std} w_{Ponkcs}}{S_{Ponkcs} \mu_{mix}} \quad (2)$$

Once ρ_{Ponkcs} is determined, the amount of each amorphous phase can be found from Eq. (1). The determined ρ_{Ponkcs} has no physical meaning but it can be used in Rietveld analysis to obtain the content of the amorphous phases.

3. Materials

3.1. Characterization of raw and calcined materials

Six different clays collected from around the world[2] were used in this study. The clay calcination was either carried out at EPFL at 800 °C

[2] Only regional details can be given due to confidential agreement with clay suppliers.

Table 1
XRF Compositions and main characteristics of calcined clays, cement and limestone.

Calcined clay	1	2	3	4	5	6	Cement	Lime-stone
Origin of clay	North America	South Asia	South America	South-east Asia	South America	South Asia		
Calcination	Flash	Furnace	Flash	Furnace	Furnace	Furnace		
	Phase composition (%)							
Metakaolin	94.2	76.8	64.4	46.5	31.7	15.0	–	–
Anatase	1.2	1.9	1.1	0.6	0.7	0.2	–	–
Hematite	–	0.2	–	10.0	1.7	3.9	–	–
Illite	–	–	1.7	–	–	36.2	–	–
Kaolinite	–	–	11.6	–	3.7	–	–	–
Mullite	4.6	–	–	1.2	–	–	–	–
Quartz	–	0.4	0.6	0.8	24.5	32.2	–	–
Rutile	–	–	–	–	4.3	1.5	–	–
Amorphous	0	20.7	20.6	40.9	33.4	11.0	–	–
	Physical properties							
$D_{v,50}$ (μm)	5.1	5.3	4.0	10.9	23.5	5.9	8.4	7.2
BET Specific surface (m^2/g)	9.6	15.3	12.9	45.7	18.5	18.7	0.9	1.8
	XRF composition (%)							
SiO_2	52.0	51.8	50.3	44.9	67.6	68.4	19.3	0.1
Al_2O_3	43.8	42.4	42.7	32.3	22.6	17.5	5.7	–
Fe_2O_3	0.3	1.9	0.6	15.4	6.1	8.9	3.6	–
CaO	–	0.1	–	1.3	0.5	0.6	63.6	55.0
MgO	–	0.1	–	0.8	–	0.7	1.6	0.2
SO_3	0.1	–	–	0.1	–	–	3.2	–
Na_2O	0.3	0.1	–	0.4	–	0.1	0.2	0.1
K_2O	0.1	0.1	0.1	0.2	0.3	2.3	1.2	–
TiO_2	1.5	2.4	1.8	2.4	1.5	0.8	0.3	–
P_2O_5	0.2	0.1	0.1	0.4	–	0.1	0.2	–
MnO	–	–	–	0.1	–	0.1	0.1	–
Others	0.1	0.2	0.2	0.2	–	0.2	0.3	–
LOI (at 950 °C)	1.5	1.0	3.6	1.7	1.4	0.5	0.8	42.6

for 1 h in a high-temperature oven or by external companies using flash or furnace calcination. Thermogravimetric Analysis (TGA) using the tangent method [24] was used on raw and calcined materials to determine the metakaolin content of calcined clays. The metakaolin content $wt\%_{metakaolin}$ was obtained according to Eq. (3) from the water loss during the dehydroxylation step of kaolinite $wt\%_{kaol\text{-}OH,\ raw}$ from approx. 400 °C to 600 °C leading to the formation of metakaolin [2, 25, 26]. $M_{kaolinite}$ (258.16 $g.mol^{-1}$) and M_{water} (18.02 $g.mol^{-1}$) refer to the molecular weights of kaolinite and water, respectively. This metakaolin value obtained has to be normalized to the final weight of the calcined clay since the sample mass does not remain constant during the calcination process. TGA was also run on calcined clays to assess the efficiency of calcination. In case of incomplete calcination, the amount of uncalcined material was subtracted based on the remaining water loss corresponding to kaolinite dehydroxylation $wt\%_{kaol\text{-}OH,\ calcined}$.

$$wt\%_{metakaolin} = wt\%_{kaol\text{-}OH,raw} \times \frac{M_{metakaolin}}{2M_{water}} \times \frac{100}{100 - wt\%_{kaol\text{-}OH,raw}} - wt\%_{kaol\text{-}OH,calcined} \times \frac{M_{metakaolin}}{2M_{water}} \quad (3)$$

For all calcined clays, the metakaolin content is indicated in Table 1. The secondary phases were quantified by XRD-Rietveld analysis. The X-ray Fluorescence chemical composition, the $D_{V,50}$ measured by Malvern laser diffraction and the specific surface measured by nitrogen adsorption using the BET model are also shown. In Table 1 are also indicated the physico-chemical properties of the cement and limestone used in this study. Limestone Durcal 5 from Omya company is used, and the Portland cement (PC) is a commercial CEM I 42.5R from Heidelberg Cement. The cement phase composition is shown in Table 2.

Table 2
Cement phase composition measured by XRD-Rietveld method.

Clinker	Content (%)	Clinker	Content (%)
C_3S	64.6	Periclase	0.8
C_2S	5.2	Arcanite	1.7
C_3A cub.	2.2	Anhydrite	5.9
C_3A orth.	5.0	Lime	0.3
C_4AF	13.8	Aphthitalite	0.5

4. Analytical details

4.1. Paste sample preparation

LC^3-50 pastes were cast using 55 parts of cement, and a combination of 30 parts of calcined clay and 15 parts of limestone. The cement used in this study contains an adequate sulfate content for a plain Portland cement hydration. For LC^3-50 blends, the addition of 2% extra gypsum (Acros, 98+ grade) was needed to avoid undersulfation, as detailed in [27]. Thus, the LC^3-50 blends were composed of 53.9% of cement (50.7% of clinker and 3.2% of anhydrite), 29.4% of calcined clay, 14.7% of limestone and 2% of gypsum addition.

A water to binder ratio of 0.4 was used for the paste casting. Pastes were mixed at 1600 rpm for 2 min. Similar workability between the different LC^3-50 blends was obtained using polycarboxylate superplasticizer. The amount of superplasticizer required increases with the metakaolin content, up to 1.4% of total solid mass. Pastes were sealed cured at 20 °C. 3 mm-thick slices for X-ray Diffraction (XRD) and Scanning Electron Microscopy (SEM) were cut at 1, 3, 7, 28 and 90 days of hydration. Fresh slices were used to carry out XRD measurements combined with the Rietveld refinement method. For SEM and XRD/PONKCS samples, isopropanol was used to stop hydration. The solvent was changed after 1 h, 1 day and 3 days. Samples were then stored in a

desiccator under vacuum for at least 3 days. For SEM, samples were then impregnated in epoxy resin and polished using sprays of diamond particles of 9, 3 and 1 μm for 20 min, 2 h and 3 h, respectively. A 15-nm carbon coating was finally applied to prevent charging effect.

4.2. Mass balance and thermodynamic modelling

4.2.1. Consumption of anhydrous phases

XRD-Rietveld analysis was used to quantify the amount of unreacted clinker phases, limestone and gypsum at 1, 3, 7, 28 and 90 days. The consumption of these phases is used as input for mass balance and thermodynamic modelling. XRD also permitted to quantify the ettringite content used for mass balance. Hemi- and monocarbonate phases were also measured to be compared with the outputs of mass balance and thermodynamic modelling. Fresh samples were used for the phase quantification by XRD-Rietveld analysis to make sure that hydrated phases do not undergo any partial dehydration due to the hydration stopping method (isopropanol and vacuum drying) [24]. XRD patterns were acquired with Bragg-Brentano mode with a X'Pert PANalytical diffractometer with CuKα radiation operated at 45 kV and 40 mA. Samples were scanned from 5 to 70°2θ with a step size of 0.0167°2θ using a X'Celerator detector. The equivalent time per step was 30 s, resulting in a total measurement time of 15 min per scan. Rutile was used as external standard.

4.2.2. Composition of clinker phases

Since clinker phases do not exactly have their stoichiometric compositions, a SEM/EDX point analysis was carried out to more precisely determine the contribution of each main oxide to the hydration reactions. The compositions of the clinker phases are shown in Table 3 and are very close to the typical values given by Taylor [28].

4.2.3. C-A-S-H composition

To determine the C-A-S-H composition used for mass balance and thermodynamic modelling calculations, a FEI Quanta 200 SEM was used with an accelerating voltage of 15 kV on polished cross-sections, with a working distance of 12.5 mm, and a spot size adjusted to get a current of approx. 0.8 nA. The determination of C-A-S-H composition was obtained by Energy Dispersive X-ray Spectroscopy (EDX) on 200 points per sample per age according to the method of Rossen [29]. In order to get a more accurate composition of C-A-S-H, inner product was selected for analysis to minimise the intermixing with other phases present in the microstructure. Fig. 2 shows an example of the significant differences in terms of Al/Ca and Si/Ca ratios for C-A-S-H for PC and LC^3-50 (46.5%) at 28 days of hydration. The small coloured symbols represent all the points analysed for each system, and the large symbols show the composition of the “pure” C-A-S-H (the least intermixed).

Table 3
Clinker phase composition determined by SEM/EDX point analysis.

	C_3S	C_2S	C_3A	C_4AF
CaO	70.68	62.07	56.68	48.50
SiO_2	24.81	31.28	4.74	4.85
Al_2O_3	1.14	1.43	28.02	18.79
Fe_2O_3	0.74	1.11	5.11	21.07
MgO	1.03	0.62	0.91	3.55
Na_2O	0.29	0.47	1.38	0.59
K_2O	0.88	1.75	2.97	0.91
SO_3	0.08	0.18	0.13	0.15
TiO_2	0.13	0.22	0.01	1.39
P_2O_5	0.22	0.87	0.05	0.22

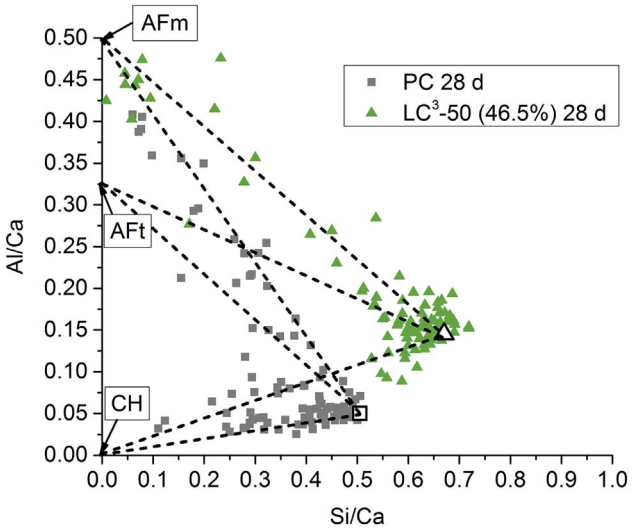

Fig. 2. Al/Ca versus Si/Ca ratio of C-A-S-H for PC and LC^3-50 (46.5%) at 28 days of hydration.

4.3. PONKCS

4.3.1. XRD data collection

For the PONKCS method, the protocol described in [16] was used. Similar parameters as Rietveld measurements were used, except the equivalent time per step which was increased to 60 s, increasing the total measurement time to 30 min per scan. Dried samples were used to get a similar background for all samples. 2 g of sample were ground for 5 min in a ceramic mortar to make sure that the particle size of the powder is similar for each test. This amount of sample was chosen to ensure a short grinding time in order to limit the potential carbonation of the hydration products. The samples were back-loaded to minimize preferred orientation. Topas-Academic v6.0 software was used to perform the Rietveld analysis.

For all tested samples, a zero-order Chebyshev polynomial accompanied by 1/x term was used to fit the background. The hump of C-A-S-H was defined from using sets of pseudo Voigt peaks on a 7-year old hydrated white cement, and the metakaolin hump was defined using one asymmetric split pseudo Voigt peak (as shown in Fig. 4(b)) [16]. The amorphous hump for metakaolin was defined on the purest metakaolin sample, specifically the calcined clay containing 94.2% of metakaolin. This metakaolin hump was then applied to the other calcined clays, after making sure that the position of the amorphous hump is similar for all calcined clays samples, as shown in Fig. 3. ρ_{Ponkcs} was then determined, using w_{Ponkcs} as the metakaolin content of each calcined clay (cf. Table 1). For a metakaolin content lower than 75% in calcined clay, amorphous impurities do not permit to get a good fit using the metakaolin hump only. Thus, a second hump (namely the impurity hump) was introduced to model the global amorphous hump of the calcined clay, as well as some short-term ordering of metakaolin structure [30]. Fig. 4(a) shows the two humps used to fit the calcined clay containing 64.4% of metakaolin. For hydrated blends, the parameters of these amorphous humps were kept fixed except the scale factor. The contribution of the C-A-S-H and the calcined clay humps to the calculated pattern for LC^3-50 (64.4%) at 28 days of hydration is shown in Fig. 4(b).

5. Results

5.1. Mass balance and thermodynamic modelling

An example of mass balance procedure and thermodynamic modelling applied to LC^3-50 (94.2%) at 28 days of hydration is shown in

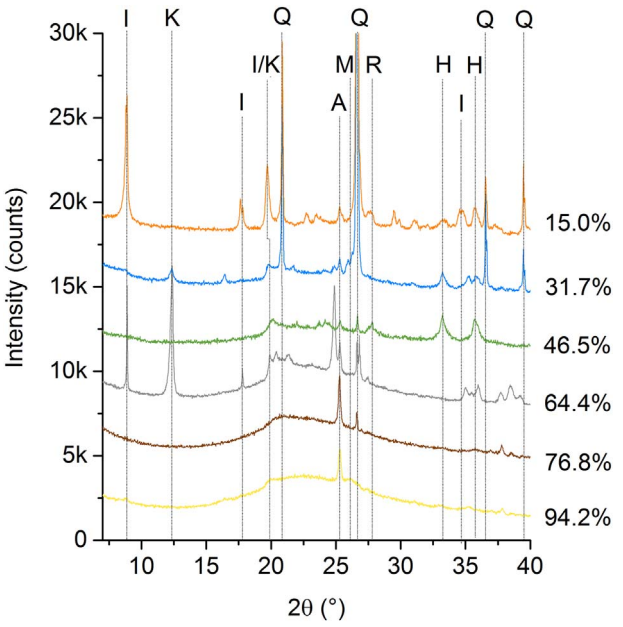

Fig. 3. XRD patterns of calcined clays. The main peaks of illite (I), uncalcined kaolinite (K), quartz (Q), mullite (M), rutile (R) and hematite (H) are indicated.

Fig. 5(a) and (b), respectively. The amount of reacted metakaolin in the calcined clay is shown up to 45% in order to focus on the range of interest (until the end of portlandite consumption). The phase assemblage predicted by both methods is very close, especially in the range from 20 to 40% of reacted metakaolin. With the increase of the amount of reacted metakaolin, portlandite gets consumed, leading to the formation of C-A-S-H and monocarboaluminate. Below 15% of reacted metakaolin, the mass balance method does not predict any formation of carboaluminate hydrates because the input of aluminium is all used to form hydrotalcite, C-A-S-H and ettringite. Hydrotalcite, hydrogarnet and ettringite contents are independent of the amount of reacted metakaolin, since their amount is limited by the availability of MgO, Fe_2O_3 and SO_3. Below 10% of reaction, thermodynamic modelling predicts a lower amount of ettringite and no carboaluminate hydrates. This is also due to the lack of aluminium in the system. Most of aluminium is used for C-A-S-H formation, based on a constant Al/Si ratio independent of the amount of reacted metakaolin. Thermodynamic modelling starts predicting strätlingite in LC^3-50 systems after complete reaction of portlandite (from 35% of reacted metakaolin onwards).

The determination of the reacted metakaolin is shown in Fig. 6 for the same system. Portlandite gets consumed as the amount of reacted metakaolin increases. The amount of reacted metakaolin is estimated from the actual portlandite content from experimental XRD-Rietveld data (horizontal line) is obtained. The grey and blue solid lines show the portlandite as a function of reacted metakaolin from mass balance and thermodynamic modelling, respectively. The dashed lines represent the experimental error of portlandite quantification by XRD-Rietveld analysis. This gives the errors on the determination of the amount of reacted metakaolin. Portlandite was also quantified by TGA. Similar results were obtained using both techniques.

Mass balance and thermodynamic modelling were applied to the different LC^3-50 systems, and the results obtained at 1, 3, 7, 28 and 90 days of hydration are shown in Fig. 7(a) and (b), respectively. It shows that at 1 and 3 days, the amount of reacted metakaolin is globally similar for all systems except for the LC^3-50 (15.0%) which is lower. From 7 days onwards, the amount of reacted metakaolin globally increases with the metakaolin content by mass balance. However, the amplitude of the increase decreases with the metakaolin content. The amount of reacted metakaolin by thermodynamic modelling is quite similar for calcined clays containing > 50% of metakaolin.

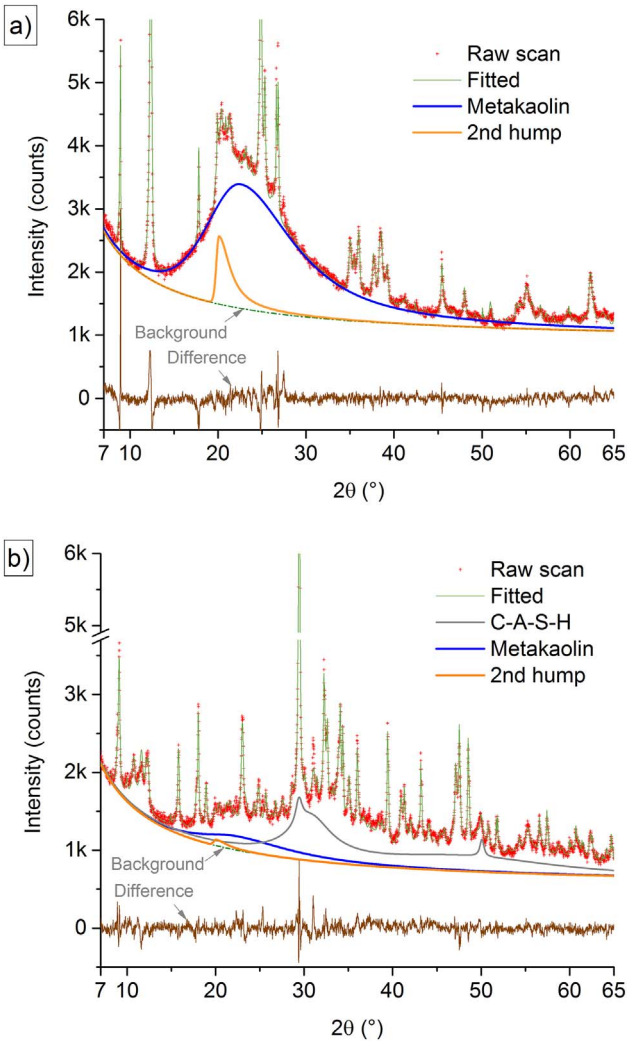

Fig. 4. Decomposition of the XRD pattern of the calcined clay containing 64.4% of metakaolin (a) and of the LC^3-50 (64.4%) at 28 days of hydration (b) with the contributions of C-A-S-H, metakaolin and the secondary hump of calcined clay.

The correlation of the amount of reacted metakaolin by mass balance and by thermodynamic modelling is shown in Fig. 8. The results obtained until 7 days are very similar between both methods. At 28 and 90 days, thermodynamic modelling predicts a slightly lower amount of reacted metakaolin. This difference could be explained by the C-S-H model used in this method. The Ca/Si ratio of C-S-H model is 1.63 ($C_{1.63}SH_{2.9}$), whereas the measured Ca/Si ratios by SEM–EDX are lower (1.49 to 1.58). Thus, more calcium is used in thermodynamic modelling for the formation of C-S-H. As a consequence, the amount of portlandite left is lower, leading to a slight decrease of the amount of reacted metakaolin.

The reaction degree of metakaolin is then calculated according to Eq. (4). It is shown in Fig. 9(a) and (b) for mass balance and thermodynamic modelling, respectively. It shows that for both methods, the reaction degree of metakaolin decreases with the metakaolin content of the calcined clay. For the calcined clay containing 15.0% of metakaolin, all metakaolin has reacted at 90 days of hydration.

$$\text{Reaction degree of metakaolin (\%)} = \frac{\text{Reacted metakaolin} \times 100}{wt\%_{\text{metakaolin}}} \quad (4)$$

5.2. Sensitivity analysis for mass balance and thermodynamic modelling

In order to estimate the influence of the errors of measurements of

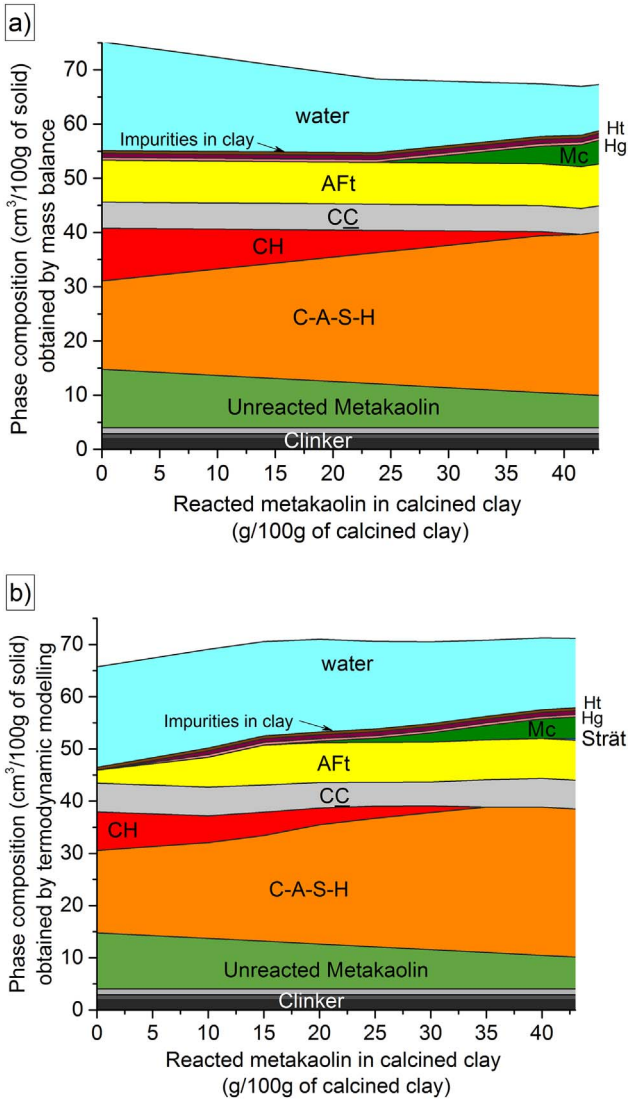

Fig. 5. Phase assemblage of LC^3-50 (94.2%) at 28 days of hydration using mass balance (a) and thermodynamic modelling (b). Ht = hydrotalcite, Hg = hydrogarnet, Mc = monocarboaluminate, AFt = ettringite, C$\underline{C}$ = unreacted calcite, CH = portlandite.

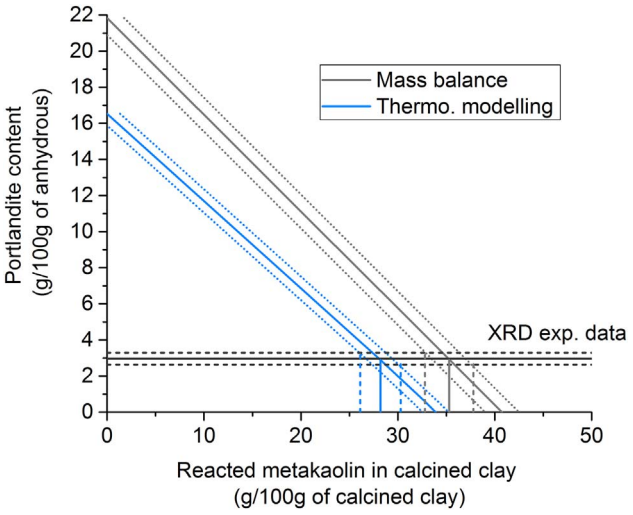

Fig. 6. Determination of the degree of reaction of metakaolin for mass balance and thermodynamic modelling example for LC^3-50 (94.2%) at 28 days of hydration.

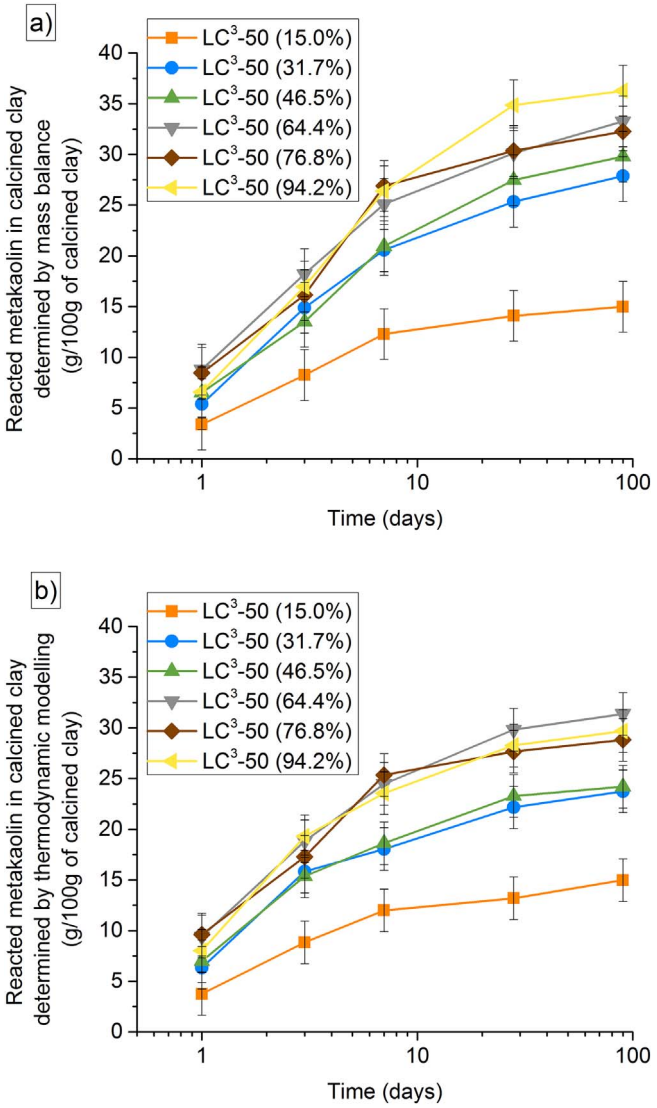

Fig. 7. Amount of reacted metakaolin for the different LC^3-50 blends at 1, 3, 7, 28 and 90 days determined by mass balance (a) and thermodynamic modelling (b).

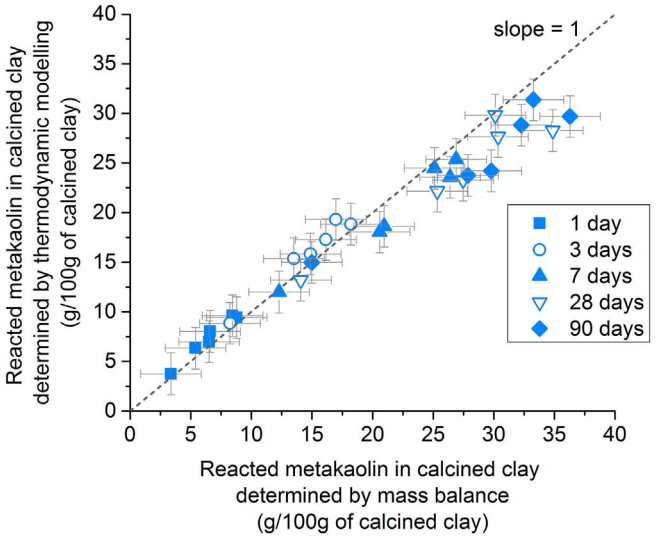

Fig. 8. Correlation between the amount of reacted metakaolin obtained by mass balance and by thermodynamic modelling

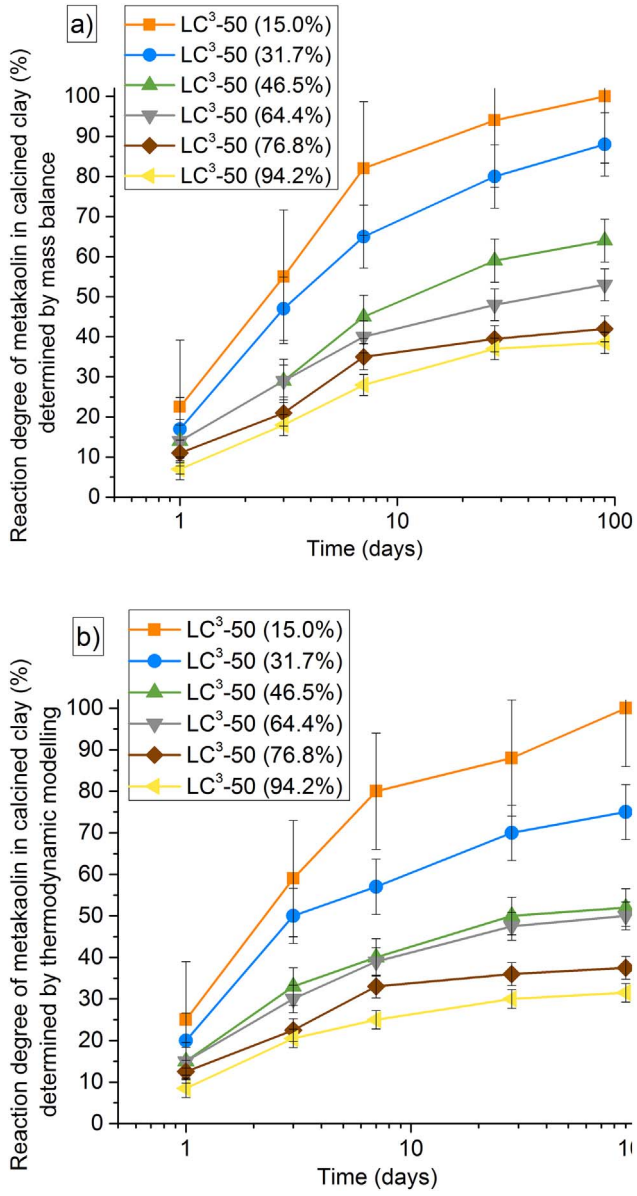

Fig. 9. Reaction degree of metakaolin for the different LC^3-50 blends at 1, 3, 7, 28 and 90 days determined by mass balance (a) and thermodynamic modelling (b).

Table 4
Error of measurement of clinker phases, C-A-S-H composition, ettringite and portlandite.

	Error (g/100 g of anhydrous)
Clinker phases (XRD-Rietveld)	± 1.0
C-A-S-H composition (SEM-EDX)	
Al/Ca	± 0.015
Si/Ca	± 0.015
Ettringite (XRD-Rietveld)	± 1.1
Portlandite (XRD-Rietveld)	± 0.4

the input data on the determination of the amount of reacted metakaolin for mass balance and thermodynamic modelling, a sensitivity analysis was carried out. Table 4 shows the error values considered for the determination of the clinker phase content, the ettringite quantification, the C-A-S-H composition and the portlandite quantification. Based on these errors, the maximum variations are applied to study their impact on the final amount of reacted metakaolin. The maximum deviation obtained for the amount of reacted metakaolin by mass balance is ± 2.5 g/100 g of calcined clay. For thermodynamic modelling, a slightly smaller deviation is obtained, ± 2.1 g/100 g of calcined clay, since ettringite content and Si/Ca ratio are not experimentally measured.

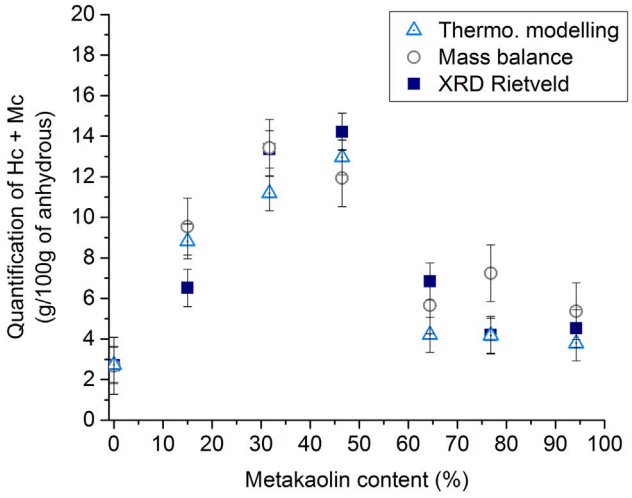

Fig. 10. Amount of carboaluminate hydrates obtained at 28 days of hydration by thermodynamic modelling, mass balance and XRD/Rietveld.

5.3. Output reliability

Since metakaolin provides SiO_2 and Al_2O_3 to the system, C-A-S-H and carboaluminate formation are mainly affected, because their formation is limited by the complete consumption of the remaining SiO_2 and Al_2O_3. For C-A-S-H formation, we do not have any precise independent method for measuring the amount. But the amount of carboaluminates formed during hydration can be compared between mass balance, thermodynamic modelling and experimental XRD-Rietveld data. For mass balance, the formation of carboaluminate hydrates corresponds to the complete consumption of the remaining aluminium after the formation of hydrotalcite, C-A-S-H and ettringite. Both hemi- (Hc) and monocarboaluminate (Mc) phases are identified for the different blends by XRD-Rietveld method. Fig. 10 shows the comparison of the sum of hemi- and monocarboaluminate hydrates between mass balance, thermodynamic modelling and XRD-Rietveld results. A good agreement is found for all calcined clay blends. The relative low content as well as the poor crystallinity of hemicarboaluminate phase is the main source of the observed differences for XRD-Rietveld results. The explanation for the trends observed, i.e. the increase of the amount of carboaluminate hydrates up to 50% of metakaolin in calcined clay and its decrease above is analysed in more details in [17].

5.4. PONKCS method

The results obtained using PONKCS method are shown in Fig. 11 for the different LC^3-50 systems. The error of measurement was determined based on three series of measurements. It shows that the amount of reacted metakaolin increases with time, but the trends are not as clear as mass balance and thermodynamic modelling. The results obtained are more spread, with higher deviations, especially for the LC^3-50 systems containing < 50% of metakaolin.

The reaction degree of metakaolin at 1, 3, 7, 28 and 90 days is shown in Fig. 12 for the different LC^3-50 systems. Due to the high scatter of the data, especially for the LC^3-50 (15.0%), clear trends cannot be obtained. As observed for mass balance and thermodynamic modelling, the reaction degree of metakaolin globally decreases with the metakaolin content of the calcined clay.

A comparison with mass balance is shown in Fig. 13. Similar values

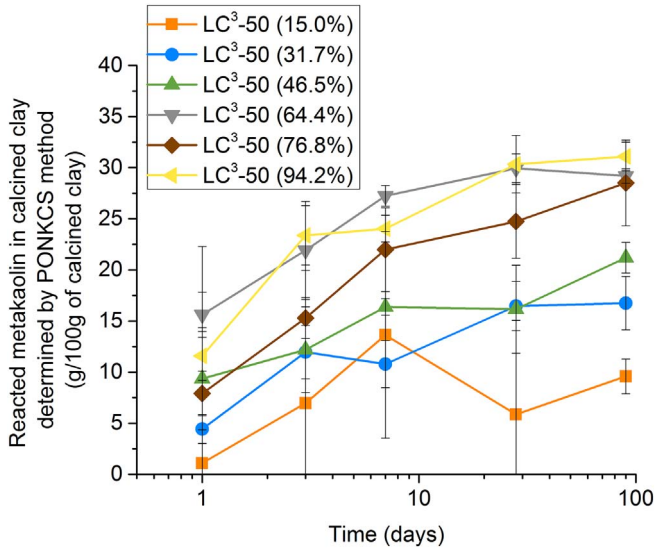

Fig. 11. Amount of reacted metakaolin at 1, 3, 7, 28 and 90 days determined by PONKCS method.

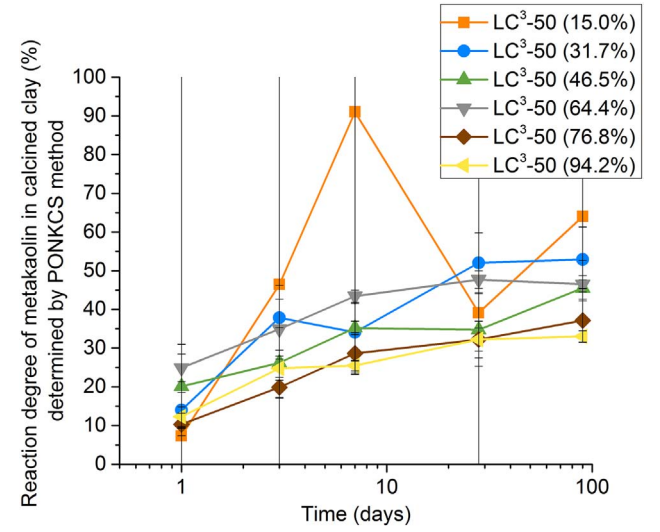

Fig. 12. Reaction degree of metakaolin at 1, 3, 7, 28 and 90 days determined by PONKCS method.

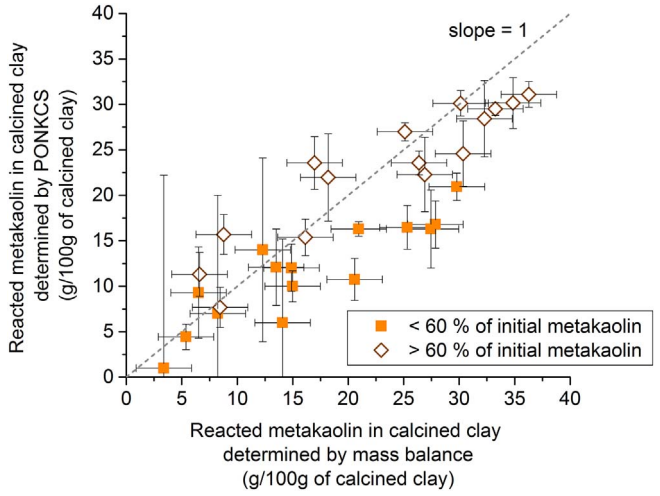

Fig. 13. Correlation between the amount of reacted metakaolin obtained by mass balance and by PONKCS.

to mass balance are reached for LC^3-50 systems with a metakaolin content higher than 60% in calcined clay, as shown by the hollow symbols. The plain symbols show the correlation for the blends containing < 60% of metakaolin in the calcined clay. The amount of reacted metakaolin obtained for blends with < 60% of metakaolin in calcined clay is lower than the values obtained by mass balance. With the decrease of the metakaolin content in the calcined clay, the measurement of the amount of reacted metakaolin becomes more challenging due to the detection limit for the PONKCS method. As example, in LC^3-50 (15.0%), the initial amount of metakaolin in the system is 4.5 g per 100 g of anhydrous binder only. During hydration, the residues of unreacted metakaolin are not easy to identify and quantify, leading to significant errors of measurement. Moreover, the impurity hump increases with the decrease of the metakaolin content of the calcined clay. The complexity of the amorphous humps also decreases the reliability of the results even if the overall fitting is improved.

Thus, the PONKCS method gives a quite reliable indication of the amount of reacted metakaolin for blends containing > 60% of metakaolin in calcined clay, i.e. with > 14 g of unreacted metakaolin left per 100 g of binder. Below this value, the precision of PONKCS method becomes poor.

6. Conclusion

Among the three methods used in this study, the mass balance approach shows the most reliable results to determine the amount of reacted metakaolin. Thermodynamic modelling is less time-consuming than mass balance since it does not necessarily require any SEM-EDX measurement and it can be run simply based on XRD-Rietveld outputs. However, despite very similar results to mass balance until 7 days of hydration, thermodynamic modelling underestimates the amount of reacted metakaolin for later ages due to the fixed Ca/Si ratio used in the model of C-S-H.

PONKCS method gives close results to mass balance and thermodynamic modelling for LC^3-50 blends containing > 60% of metakaolin in the calcined clay. However, this method gives higher deviations in the results, especially for blends containing calcined clays with < 60% of metakaolin. Below 60% of metakaolin, the quantification becomes very complex due to the small amount left of unreacted metakaolin.

The three methods show that the amount of reacted metakaolin increases with time and that this amount is globally higher for a higher metakaolin content in the calcined clay. However, the increase of reacted metakaolin with the metakaolin content becomes less important for high-grade calcined clays.

Acknowledgments

Financial support from Swiss Agency for Development and Cooperation (SDC) grant number 81026665 is acknowledged by the authors.

References

[1] K. Scrivener, J. Vanderley, E. Gartner, Eco-efficient Cements: Potential, Economically Viable Solutions for a Low-CO_2, Cement Based Materials Industry, UNEP, Karen L. Scrivener, Vanderley M. John, Ellis M. Gartner, 2016.
[2] R. Fernandez, F. Martirena, K.L. Scrivener, The origin of the pozzolanic activity of calcined clay minerals: a comparison between kaolinite, illite and montmorillonite, Cem. Concr. Res. 41 (2011) 113–122.
[3] C. He, B. Osbaeck, E. Makovicky, Pozzolanic reactions of six principal clay minerals: activation, reactivity assessments and technological effects, Cem. Concr. Res. 25 (1995) 1691–1702.
[4] S. Hollanders, R. Adriaens, J. Skibsted, Ö. Cizer, J. Elsen, Pozzolanic reactivity of pure calcined clays, Appl. Clay Sci. 132 (2016) 552–560.
[5] J. Ambroise, M. Murat, J. Péra, Hydration reaction and hardening of calcined clays and related minerals. V. Extension of the research and general conclusions, Cem. Concr. Res. 15 (1985) 261–268.
[6] K.L. Scrivener, Options for the future of cement, Indian Concr. J. 88 (2014) 11–21.
[7] K.L. Scrivener, B. Lothenbach, N. De Belie, E. Gruyaert, J. Skibsted, R. Snellings,

A. Vollpracht, TC 238-SCM: hydration and microstructure of concrete with SCMs, Mater. Struct. 48 (2015) 835–862.
[8] Z.T. Dai, T. Thuan, J. Skibsted, Aluminum incorporation in the C-S-H phase of white Portland cement-metakaolin blends studied by 27Al and 29Si MAS NMR spectroscopy, J. Am. Ceram. Soc. 97 (2014) 2662–2671.
[9] W. Kunther, Z. Dai, J. Skibsted, Thermodynamic modeling of hydrated white Portland cement–metakaolin–limestone blends utilizing hydration kinetics from 29 Si MAS NMR spectroscopy, Cem. Concr. Res. 86 (2016) 29–41.
[10] Z. Shi, M.R. Geiker, K. De Weerdt, T.A. Østnor, B. Lothenbach, F. Winnefeld, J. Skibsted, Role of calcium on chloride binding in hydrated Portland cement–metakaolin–limestone blends, Cem. Concr. Res. 95 (2017) 205–216.
[11] S.L. Poulsen, V. Kocaba, G. Le Saoût, H.J. Jakobsen, K.L. Scrivener, J. Skibsted, Improved quantification of alite and belite in anhydrous Portland cements by 29Si MAS NMR: effects of paramagnetic ions, Solid State Nucl. Magn. Reson. 36 (2009) 32–44.
[12] E.M.J. Berodier, Impact of the Supplementary Cementitious Materials on the Kinetics and Microstructural Development of Cement Hydration, EPFL, 2015.
[13] M. Antoni, J. Rossen, F. Martirena, K. Scrivener, Cement substitution by a combination of metakaolin and limestone, Cem. Concr. Res. 42 (2012) 1579–1589.
[14] P.T. Durdziński, M. Ben Haha, S.A. Bernal, N. De Belie, E. Gruyaert, B. Lothenbach, E. Menéndez Méndez, J.L. Provis, A. Schöler, C. Stabler, Z. Tan, Y. Villagrán Zaccardi, A. Vollpracht, F. Winnefeld, M. Zając, K.L. Scrivener, Outcomes of the RILEM round robin on degree of reaction of slag and fly ash in blended cements, Mater. Struct. 50 (2017) 135.
[15] P.T. Durdziński, M. Ben Haha, M. Zajac, K.L. Scrivener, Phase assemblage of composite cements, Cem. Concr. Res. 99 (2017) 172–182.
[16] R. Snellings, A. Salze, K.L. Scrivener, Use of X-ray diffraction to quantify amorphous supplementary cementitious materials in anhydrous and hydrated blended cements, Cem. Concr. Res. 64 (2014) 89–98.
[17] F. Avet, K. Scrivener, Investigation of the Calcined Kaolinite Content on the Hydration of Limestone Calcined Clay Cement (LC3) Submitted, (2017).
[18] P. Durdzinski, Hydration of Multi-component Cements Containing Cement Clinker, Slag, Calcareous Fly Ash and Limestone, Ecole Polytechnique Fédérale de Lausanne, Thesis n°6834, (2016).
[19] B.Z. Dilnesa, E. Wieland, B. Lothenbach, R. Dähn, K.L. Scrivener, Fe-containing phases in hydrated cements, Cem. Concr. Res. 58 (2014) 45–55.
[20] Available at, 2014. http://gems.web.psi.ch, .
[21] Available at http://www.empa.ch/cemdata Cemdata 14, EMPA, 2014.
[22] D.A. Kulik, Improving the structural consistency of C-S-H solid solution thermodynamic models, Cem. Concr. Res. 41 (2011) 477–495.
[23] A.C.A. Muller, K.L. Scrivener, A.M. Gajewicz, P.J. McDonald, Densification of C-S-H measured by 1H NMR relaxometry, J. Phys. Chem. C 117 (2013) 403–412.
[24] K. Scrivener, R. Snellings, B. Lothenbach, A Practical Guide to Microstructural Analysis of Cementitious Materials, Taylor & Francis, 2016.
[25] P. Ptáček, F. Frajkorová, F. Šoukal, T. Opravil, Kinetics and mechanism of three stages of thermal transformation of kaolinite to metakaolinite, Powder Technol. 264 (2014) 439–445.
[26] A. Shvarzman, K. Kovler, G.S. Grader, G.E. Shter, The effect of dehydroxylation/amorphization degree on pozzolanic activity of kaolinite, Cem. Concr. Res. 33 (2003) 405–416.
[27] F. Avet, R. Snellings, A. Alujas Diaz, M. Ben Haha, K. Scrivener, Development of a new rapid, relevant and reliable (R3) test method to evaluate the pozzolanic reactivity of calcined kaolinitic clays, Cem. Concr. Res. 85 (2016) 1–11.
[28] H.F.W. Taylor, Cement Chemistry, Thomas Telford, 1997.
[29] J. Rossen, Composition and Morphology of C-A-S-H in Pastes of Alite and Cement Blended with Supplementary Cementitious Materials, Ecole Polytechnique Fédérale de Lausanne, Thesis n°6294, (2014).
[30] S. Lee, Y.J. Kim, H.-S. Moon, Energy-filtering transmission electron microscopy (EF-TEM) study of a modulated structure in metakaolinite, represented by a 14 Å modulation, J. Am. Ceram. Soc. 86 (2003) 174–176.